Photostimulated exoemission and reduction of CeO_2

I. V. Krylova

Department of Chemistry, M. V. Lomonosov Moscow State University, Leninskie Gory, 119899 Moscow, Russian Federation. Fax: +7 (095) 932 8846

The thermovacuum and photochemical reduction of CeO_2 was studied by the method of photostimulated exoemission. Analysis of the kinetics and temperature dependence of photostimulated exoemission permits one to suggest a possible mechanism of electron and ion phenomena accompanying the reduction processes.

Key words: cerium dioxide, reduction, photostimulated exoemission.

Cerium dioxide and related catalytic systems are widely used in three-route converters for neutralization of automobile exhaust. It is known that CeO_2 is used as an active component of catalysts for CO and CH_4 oxidation.[1,2] Cerium dioxide is active in the partial oxidation of CH_4 to synthesis gas, and platinum additives considerably increase the rate of formation of H_2 and CO.[3] Copper-modified cerium dioxide is active in the reduction of SO_2 by carbon monoxide.[4] The high activity of CeO_2 in redox reactions is attributed to the ability of its crystals with the fluorite structure to be reduced rather easily, forming mobile oxygen vacancies.[5] The chemistry of defects in the CeO_2 bulk has been rather well studied.[6] It has been shown that the oxygen vacancies formed during the reduction are initially doubly ionized, and at greater deviations from stoichiometry they are singly ionized. Electrons released in the formation of the vacancies possess a high mobility and can migrate to the localized C(4f) centers.[7] It is assumed[8] that these quasi-free electrons are responsible for the formation of the surface O_2^- and O_2^{2-} ions during adsorption. The active surface oxygen, for example, in the form of O_2^-, participates in deep oxidation of hydrocarbons (electrophilic reactions), whereas the lattice oxygen is responsible for partial oxidation of hydrocarbons (nucleophilic reactions). The development of catalysts with specified oxidation properties requires monitoring the nature of intermediate forms of active oxygen.[7]

Unlike volume defects, data on the energy parameters of formation and other characteristics of surface defects of CeO_2 are scarce.[1] Exoemission, *viz.* the low-temperature (4—700 K) nonstationary emission of electron and ions, arises from mechanical (thermomechanical) actions, radiation, or physicochemical processes on a solid surface and are sluggish.[9,10] The thermostimulated emission (TSE) characterized by several peaks (T_{max}) occurs after a decrease in the emission current to the background value on heating in a linear regime. The positions of peaks in the temperature scale represent an energy spectrum of defects that are the levels of electron localization on the solid surface. Photostimulated emission (PSE) is observed under irradiation with light in the wavelength region exceeding the photoeffect threshold (ultraviolet irradiation, UVI). It is assumed that the shift of the photoeffect threshold towards the long-wave region is due to the presence of defects formed by the preliminary action. Exoemission (TSE, PSE) occurs from the superficial (≤10 nm) surface layer of solids and makes it possible to study the formation of the physical and chemical defects on the surface.

The mechanism of PSE presently appears to be speculative.[11] Defects of the type of color centers are assumed to be the PSE source. However, many PSE phenomena cannot be explained in the framework of this model. It is known that UVI results in the photoactivation of the surface accompanied by such phenomena as photoadsorption, photodesorption, photocatalysis, photochemical decomposition, *etc.*[12] Electronic and atomic-molecular processes on photoactivated solid surfaces (semiconductors and dielectrics) have previously[13] been studied in detail. However, simultaneous studies of the PSE phenomena and physicochemical surface processes are lacking. These studies started in the work[14] where PSE was detected in the thermovacuum and photochemical reduction of MnO_2. It has been shown that the data on the kinetics and temperature dependence of PSE make it possible to analyze electronic phenomena in the reduction of MnO_2 under thermovacuum and photochemical treatments; the formation, population, and destruction of electron-capturing levels, and dynamic phase transitions on the surface.

The study of PSE, taking into account the available data on the absorption spectra and the possible charge phototransfer in transition metal oxides, favors understanding of the mechanism of redox processes, including heterogeneous catalytic processes occurring with electron and ion transfer. The purpose of this work is to study the spectral and temperature dependences of PSE

Translated from *Izvestiya Akademii Nauk. Seriya Khimicheskaya*, No. 5, pp. 838—844, May, 2000.

1066-5285/00/4905-0836 $25.00

during the reduction of CeO_2 under thermovacuum treatment and UVI.

Experimental

Powdered CeO_2 was prepared by precipitation from an aqueous solution of $Ce(NO_3)_3$ with sodium hydrocarbonate.* The sample was dried at 150 °C and calcined for 3 h in air at 500 °C. The sample was stored in air for 6 months. Measurements of PSE were carried out *in vacuo* (~10^{-4} Pa) using detection in the pulse mode on a VEU-6 secondary electronic amplifier. When a positive potential was applied to the input of the detector, the emission of negative charges was detected. The detailed scheme of the setup has been described previously.[10] For the irradiation of the sample, a quartz window was mounted into the measuring chamber. The radiation of a DRT-230 mercury-quartz lamp and a set of narrow-band filters in the wavelength interval λ = 578—257 nm were used. Thermostimulation in the linear or stepwise (fractional) regimes was performed by a furnace placed along with a thermocouple on an external side of a sample holder. The weighed sample of CeO_2 was 50 mg.

Preliminary experiments with transition metal oxides (CeO_2, CuO, MnO_2, and manganate-based spinel) showed that cooling under certain conditions results in the appearance of maxima in the PSE intensity, which are probably due to exothermic phase transitions in the bulk or on the sample surface. Using the procedure applied by us to the study of MnO_2,[14] we studied the spectral characteristics and kinetic regularities of PSE during stepwise cooling of CeO_2. First the oxide surface was reduced by the repeated cycles including heating to 360 °C and cooling to ~20 °C with simultaneous UVI. The investigation procedure was as follows. After evacuation of the sample, the PSE excitation spectra were recorded, and then the sample was heated in a linear regime with detection of the "spontaneous" TSE and gas release. Then the sample was cooled in a stepwise regime, detecting at specified temperatures (360, 240, 175, 140, 100, and 20 °C) the kinetics of PSE at different UV wavelengths. When two testing cycles were completed, the kinetics of PSE was studied during both stepwise heating and cooling. After a series of experiments in the heating—cooling regime, the setup was switched-off overnight, evacuation was stopped, and the sample was stored for 16 h under the static vacuum conditions (air, $p \approx 10^{-5}$—10^{-4} Torr). During this time, both adsorption of gases due to the deterioration of a vacuum and diffusion of weakly bound oxygen from the near-surface layers of the sample to the surface can occur. Due to this, when a voltage was applied to the detector, an increased "background," *i.e.*, the emission of negative charges slowly descending in time, was observed and then the PSE excitation spectra were recorded at ~20 °C. Then the second testing cycle was carried out according to the above described procedure.

In the next experiments, the photothermostimulated emission (PTSE) was detected on heating of the sample in a linear regime and simultaneous UVI with λ = 365 nm corresponding to the PSE threshold. The heating rate was 10 K min^{-1}.

Results and Discussion

Spontaneous TSE. Figure 1 shows the spontaneous TSE from the surface of the initial CeO_2 sample due to its pre-treatment under the conditions of catalyst preparation (calcination in air at 500 °C) and storage in air for 6 months. When a positive potential is applied to the input of the detector, a slowly decaying low-intensity emission is observed, indicating the presence of weakly bound negative charges on the surface. Subsequent heating results in the appearance of small peaks at temperatures of 80—130, 175, and 240 °C and a strong splash of emission current at 275 °C.

We have previously shown[9,10] that the spontaneous TSE of metals, semiconductors, and oxides is mainly observed after their treatment in moist media (corrosion, etching, annealing in moist gases, in particular, annealing of metals in moist hydrogen) or during storage in air of hydrophilic compounds and is the result of desorption of OH^- anions. For compounds containing weakly bound oxygen, for example, high-temperature superconductors Y—Ba—Cu—O, spontaneous emission is due to the desorption of charged oxygen species in the form of O_2^-, O^-, and others. Since CeO_2 possesses a high oxidative catalytic activity and capability of absorbing and retaining oxygen, the spontaneous TSE should be attributed, in this case, to charged oxygen species (see also Ref. 8).

The emission current peaks are accompanied by splashes of gas release. Since the experiments were carried out under a dynamic vacuum, the thermodesorption peaks were manifested when the gas release rate exceeded the evacuation rate and the pressure was changed within 10^{-6}—10^{-5} Torr. Previously we have shown that for porous and powdered samples of oxides the temperature exoemission peaks (both spontaneous and due to the pre-treatment (irradiation, mechanical treatment, *etc.*) named "excitation") coincide with the peaks of thermodesorption rate.[16] Unlike the spontane-

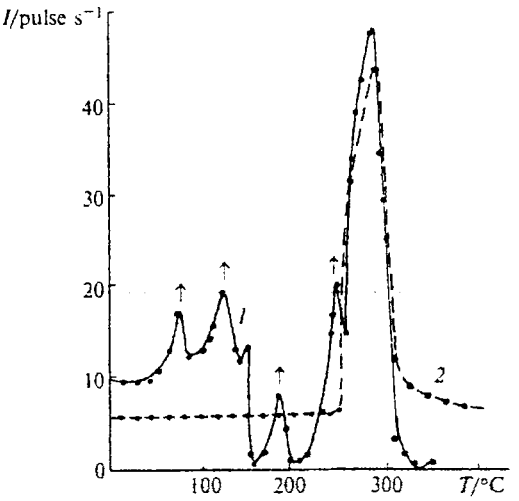

Fig. 1. Spontaneous TSE from the initial CeO_2 surface on the first (*1*) and the second (*2*) temperature-programmed heating. A sharp increase in the pressure is shown by arrows. (Hereinafter *I* is the intensity.)

* The CeO_2 sample was prepared by T. V. Simon[15] (D. I. Mendeleev Russian Chemico-Technological University), with a specific surface of 10 $m^2 g^{-1}$.

ous emission, the radiation-induced emission is observed for all the inorganic and organic materials.[9,10] It has been established[10] that TSE of ions is responsible only for a minor (10^{-6}) fraction of thermodesorbing molecules.

Characteristically, the sharp splash of emission current at 275 °C is also observed in the second cycle of runs (see Fig. 1, curve *2*), which indicates the high sorption capacity of CeO_2 with respect to oxygen. It is noteworthy that neither MnO_2[14] nor CuO[22] prepared and studied under the same conditions exhibit spontaneous emission, *i.e.*, contain no charged forms of adsorbed gases.

According to our data,[9,10,16] the indicated TSE peaks (see Fig. 1) are characteristic of most metals, semiconductors, and oxides and are due to transformations in the surface layers of oxygen species in different charge states, *i.e.*, in different oxidation degrees.

Adsorption of O_2 on the evacuated and partially reduced CeO_2 has been studied previously.[8] In the IR spectra of $^{18}O_2$ adsorbed on the evacuated surface we observed bands attributed to the superoxide radical ions O_2^-, and those for the partially reduced CeO_2 were attributed to O_2^- and peroxide anions O_2^{2-}. It is assumed that dioxygen is adsorbed in the form of O_2^- on the coordinationally unsaturated Ce^{4+} ions, whereas the O_2^{2-} form is adsorbed on a pair of Ce^{3+} ions formed during reduction.

The charged forms of oxygen are considered[8] as intermediate species that arise during dissociative adsorption of O_2 according to Scheme 1.

Scheme 1

$$O_2(ads) \xrightarrow[\text{Reduction}]{\text{Oxidation}} O_2^-(ads) \rightarrow O_2^{2-}(ads) \rightarrow 2\,O^-(ads) \rightarrow 2\,O^{2-}(lat)$$

The formation of different forms of oxygen depends on the electron-donor ability of the surface and the presence of centers stabilizing these species. It has been established[8] that O_2^{2-} anion is stable on the partly reduced surface even at $T > 150$ °C. Scheme 1 has been proposed[9,10] to attribute the peaks of TSE to the excited surface of oxides with different natures. This scheme is commonly accepted. According to the published data,[12] the temperature of 140 °C corresponds to the transformation $O_2^- \rightarrow O^-$, whereas the transition $O^- \rightarrow O^{2-}$(lat) occurs at 285 °C. In the first case, the O_2^- ions are desorbed, and in the second case, these are the O^- ions. Cerium dioxide prepared by coprecipitation from aqueous solutions and calcined in air is the stoichiometric oxide.[7] Oxygen vacancies and weakly bound electrons form during reduction. However, our data on TSE (see Fig. 1) indicate that weakly bound electrons and oxygen in the negatively charged form are also present in the near-surface layer of the initial stoichiometric CeO_2 calcined in air at 500 °C. It also follows from Fig. 1 that the chosen temperature of studying the PSE kinetics during stepwise cooling of CeO_2 coincides with the peaks of TSE and thermodesorption of different forms of weakly bound oxygen.

Spectral characteristics of PSE. The spectra of PSE excitation for the initial CeO_2 (curve *1*) and also after two (curve *2*) and four (curve *3*) cycles of the heating—cooling runs with simultaneous UVI are presented in Fig. 2. The nonselective photoeffect with a threshold near $\lambda = 365$ nm is observed for the initial stoichiometric CeO_2. After the first cycle, the shape of the curve does not change substantially (it is not shown in Fig. 2), but the PSE intensity at $\lambda = 257$ nm increases significantly (by an order of magnitude). The selective photoeffect with $\lambda_{max} = 313$ nm appears after two cycles. The absorption spectra for Ce^{3+} ions in the CaF_2 matrix are presented in the monograph.[17] Two absorption bands with $\lambda_{max} = 310$ and 335 nm were observed in the UV region. At the same time, it has been shown[13] by photoelectron spectroscopy for high-temperature superconducting cuprates containing weakly bound oxygen that in the bond energy region of $E_b = 4$ eV ($\lambda = 313$ nm) the photoemission occurs from orbitals belonging to oxygen atoms.

The PSE centers can be formed either by oxygen vacancies (Ce^{3+} ions) whose number increases with the photo- and thermovacuum reduction or by species of weakly bound oxygen whose number decreases due to the reductive treatment of CeO_2. To solve this problem, we studied the effect of thermocycling and "overnight" storage on the emission intensity. The results are presented in Tables 1 and 2.

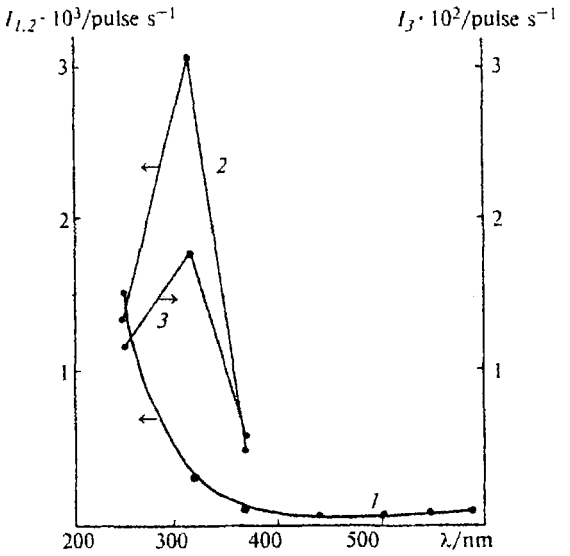

Fig. 2. Excitation spectra of PSE from the initial CeO_2 surface (*1*) after two (*2*) and four (*3*) heating—cooling cycles of runs.

Table 1. Influence of thermocyclic runs and overnight storage on the PSE intensity (I) (T = 20 °C)

λ/nm	I/pulse s^{-1}				
	Initial CeO_2	First cycle	Second cycle	After storage overnight	Fourth cycle
365	38	76	450	345	60
313	280	560	3000	2400	170
257	1480	12900	1380	13700	124

Table 2. Influence of thermocyclic runs on the PSE intensity (I) during cooling

λ/nm	T/°C	I/pulse s^{-1}		
		Ffirst cycle	Second cycle	Third cycle
365	275	170	420	880
313	275	400	1025	1415
257	275	7000	4100	415
365	140	74	370	890
313	140	190	1170	1140
257	140	3230	1300	85

Let us denote the PSE centers UV-excited at λ = 365, 313, and 257 nm by I, II, and III, respectively. Analysis of the data in Table 1 shows that the reduction of the surface results in an increase in the PSE intensity under UVI in the regions of λ = 365 and 313 nm (centers I and II) and the "overnight" storage has almost no effect on PSE. By contrast, centers III are very sensitive to the effect of thermal treatment and adsorption of residual gases ("overnight" storage). PTSE was detected under continuous UVI during linear heating and cooling of the sample. This results in more active processes of photochemical reduction of the surface than in the previous experiments. The loss of low-coordination surface oxygen and formation of CeO_{2-x} oxide with higher x are observed. Since this is precisely the oxygen which forms, according to our data, the PSE centers, the emission intensity decreases due to PTSE by 1—2 orders of magnitude at all wavelengths. According to the published data,[5] stoichiometric CeO_2 pretreated in an oxygen atmosphere at 650 °C begins to lose the lattice oxygen during heating in the 5%H_2 + He atmosphere only at 300 °C, being reduced to $CeO_{1.99}$ at 300 °C and to $CeO_{1.98}$ at 400 °C.

It has been shown[6] that at elevated temperatures and reduced oxygen pressures CeO_2 loses oxygen to become a semiconductor of the n-type. At T > 680 °C its composition changes to $CeO_{1.72}$. Using the measurement of the electroconductivity and X-ray phase analysis, the authors have found that a series of strictly specified intermediate phases Ce_nO_{2n-2} exist at lower temperatures. At slight deviations from stoichiometry, the reduction of CeO_2 is described by the following reactions[6]:

$$O_0 \longrightarrow V_O{\cdot\cdot} + 2\,e + 1/2\,O_2(g), \quad (1)$$

$$V_O{\cdot} \longrightarrow V_O{\cdot\cdot} + e, \quad (2)$$

$$V_O \longrightarrow V_O{\cdot} + e, \quad (3)$$

where O_0 is the initial stoichiometric CeO_2, $V_O{\cdot\cdot}$ is the doubly ionized vacancy, and $V_O{\cdot}$ is the vacancy with an electron localized on it.

The electroconductivity of CeO_2 has previously[18] been measured *in situ* during reduction in a hydrogen atmosphere with temperature-programmed heating. It was established that the electronductivity increased and CeO_2 was reduced to form anionic vacancies containing weakly bound electrons in the 300—773 K temperature interval. It follows from the aforesaid that the number of oxygen vacancies, Ce^{3+} ions, and weakly bound electrons increases during thermal runs in a vacuum, and the number of lattice surface oxygen O^{2-}(lat) decreases. The PSE intensity increases for centers I and II and decreases for centers III (see Table 2). It can be assumed that the PSE centers appearing under UVI with λ = 365 (I) and λ = 313 nm (II) are oxygen vacancies with the localized electrons (Ce^{3+} ions), whereas under UVI with λ = 257 nm, we observe O^{2-}(lat) ions that are present on the surface and have a lower coordination number (III). Meanwhile, the oxygen released due to photodesorption (photochemical decomposition of the CeO_2 surface) is partially localized near the formed vacancies and remains on the surface in a charged form due to the increased capability of CeO_2 to retain oxygen.[1] This can also result in an increase in the PSE intensity (λ = 365 and 313 nm) during thermocycling (see Tables 1 and 2).

Kinetics of PSE. In the first cycle of runs, the kinetic PSE curves had a smooth rise at all UVI wavelengths. The PSE kinetics in the second and third cycles are presented in Fig. 3, *a* and *b*, respectively. In the second cycle, the intensity increased in time under irradiation at λ = 365 and 313 nm and decreased under UVI with λ = 257 nm. At a higher degree of reduction in the third cycle, the intensity increased only under UVI with λ = 365 nm.

The photocurrent increases when the rate of electron accumulation on the traps formed during reduction (levels of electron localization) exceeds the rate of their decay or electron loss, for example,

$$Ce^{4+} + 2\,O^{2-}(s) \longrightarrow Ce^{3+} + 2\,O^{-}(ads) + e + V_O{\cdot}\ldots(4)$$

where O^{2-}(s) is the mobile surface (adsorbed) oxygen, and reaction (4) is the electron phototransfer. The emission increases due to either accumulation of O^- centers (centers I) in reaction (4) followed by recombination according to equation (5)

$$2\,O^- \longrightarrow O_2^- + e, \quad (5)$$

or accumulation of $V_O{\cdot}$ vacancies (centers II) in reaction (6)

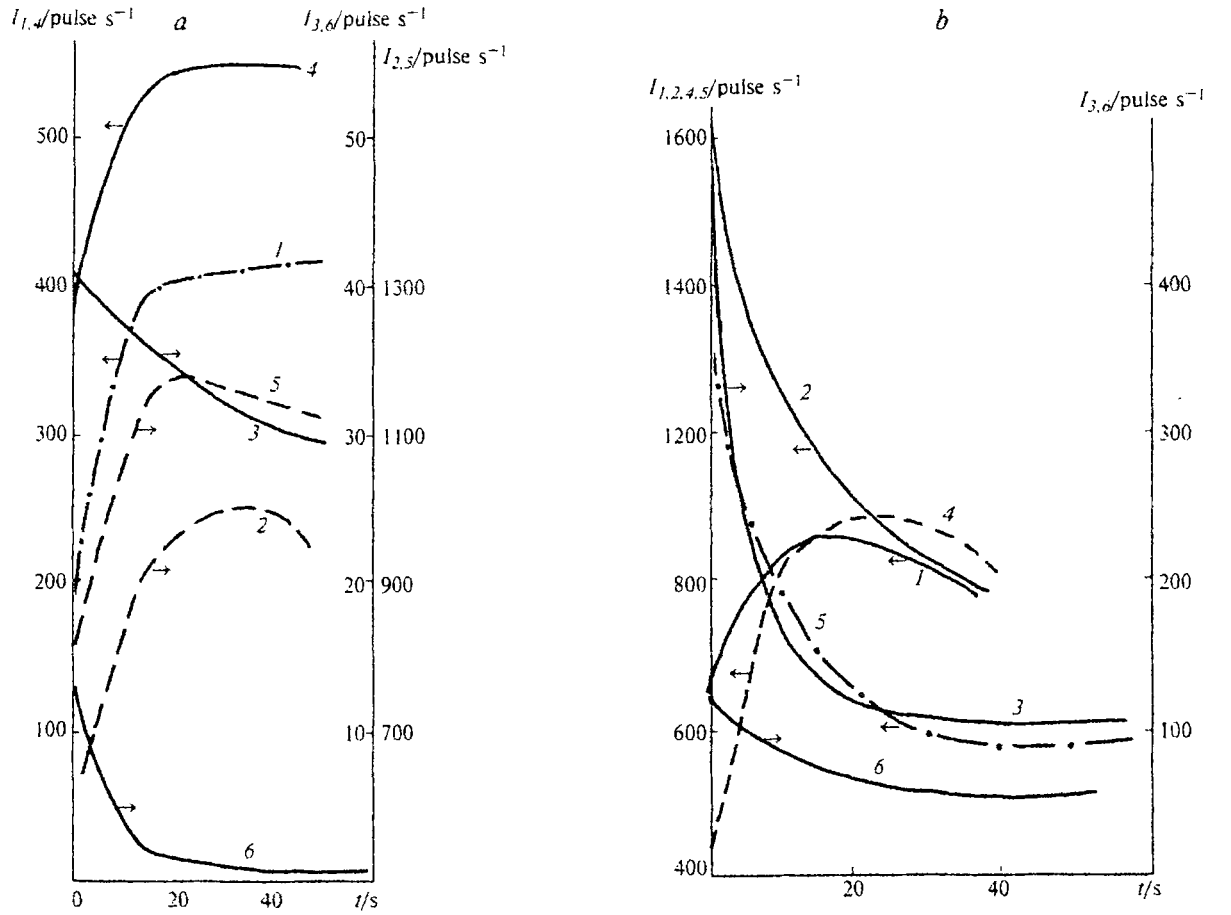

Fig. 3. Kinetics of PSE from the CeO_2 surface (*a*, the second cycle: *b*, the third cycle) during stepwise cooling at 275 °C (*1*—*3*) and 140 °C (*4*—*6*) under UVI with λ = 365 (*1*, *4*), 313 (*2*, *5*), and 257 nm (*3*, *6*).

$$V_O^{\cdot\cdot} + e \longrightarrow V_O^{\cdot} \qquad (6)$$

followed by photoionization according to reaction (2).

Centers I and II (O^-(ads) and $V_O^{\cdot}$) are connected with centers III (O^{2-}(lat)) because the increase in PSE under UVI with λ = 365 and 313 nm is accompanied by a simultaneous decrease in the emission under irradiation with λ = 257 nm (see Fig. 3, *a*). We believe that UVI with λ = 257 nm results in the direct photoionization of O^{2-}(lat) centers

$$O^{2-}(lat) \longrightarrow 1/2\ O_2 + 2\ e. \qquad (7)$$

The probability of photon absorption in the near-UV region increases with decreasing coordination number of surface oxygen.[19]

According to the published data,[6] the number of singly ionized vacancies $V_O^{\cdot}$ increases with the reduction of CeO_2 so that the increase in PSE at λ = 365 nm can be related to the formation of these vacancies in the third cycle (reactions (4), (6)). At the same time, the mobility and, hence, the recombination rate of the O^- species (reaction (5)) increase, and in the third cycle of runs, the emission intensity decreases in time under UVI with λ = 313 nm.

Temperature dependence of PSE. The temperature dependences of the PSE intensity (*I*) during stepwise cooling are presented in Fig. 4, *a*, *b*. In the first cycle, UVI with λ = 365 and 313 nm results in a monotonic decrease in the PSE intensity. Meanwhile, in the case of UVI with λ = 257 nm, slight maxima of the PSE intensity are observed at 270 °C and 140—100 °C, indicating phase transitions on the surface and the formation of emission centers. The reduction of oxide to form the intermediate Ce_nO_{2n-2} phases (see Ref. 6) is accompanied by transformations of the charged forms of weakly bound oxygen appearing according to Scheme 1 and, according to our data (see Fig. 4), by electron emission. Previously,[20] using XPS and high-energy electron loss spectra, the reactivity of chemisorbed oxygen on the metal surface has been shown to be defined by the presence of transition $O^{\delta-}$(s) and $O_2^{\delta-}$(s) states. An analogy between the state of the oxygen layers adsorbed on the metal surface and the deficient oxide surface also covered by the charged O^-, O_2^-, and O_2^{2-} forms has been shown.

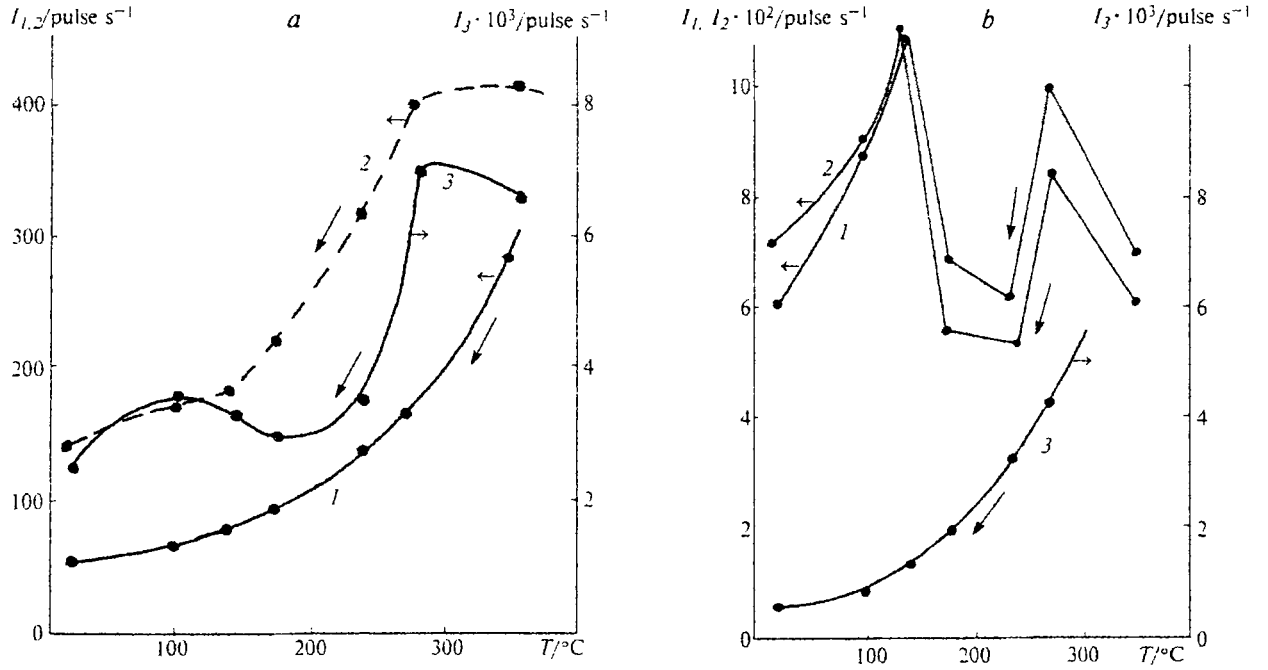

Fig. 4. Temperature dependence of the PSE intensity (*a*, first cycle; *b*, second cycle) during stepwise cooling (shown by arrows) under UVI with λ = 365 (*1*), 313 (*2*), and 257 nm (*3*).

The T_{max} temperatures on curve *3* (see Fig. 4, *a*) coincide with the TSE peaks on heating of the initial CeO_2 (see Fig. 1), which we attribute to the thermodesorption of ions of weakly bound oxygen[12] in the forms of O_2^- and O^-. According to the published data,[12] oxygen is desorbed from oxides in the O_2^- form at $T \leq 185$ °C and in the O^- form at $T > 225$ °C (T_{max} = 285 °C).[21]

In the second cycle (see Fig. 4, *b*) during cooling, distinct peaks of PSE intensity at 140 and 275 °C are observed under UVI with λ = 365 and 313 nm, whereas PSE monotonically decreases under irradiation at λ = 257 nm. During thermovacuum treatment, the reduction of the surface CeO_2 layer and the formation of vacancies and weakly bound oxygen are accompanied by the emission of negative charges. The above considered phototransfer processes (4) occurring under milder UV radiation (λ = 365 nm) are, most likely, facilitated in the partially reduced surface layer (the second testing cycle).

The results of PSE detection in the third cycle of runs during stepwise heating and cooling (curves *1* and *2*) are presented in Fig. 5. Comparison of these data indicates a hysteresis due to the formation of a new phase (Ce_nO_{2-n}) on the surface. Singly ionized oxygen vacancies (Ce^{3+} ions), whose number increases with reduction, are, most likely, the origin of emission.[6] We have previously observed[14] the hysteresis phenomena for MnO_2 during detection of PSE under similar conditions of thermovacuum reduction.

In the fourth cycle (see Fig. 5, curves *3*, *4*), no hysterisis phenomena were observed in the detection of

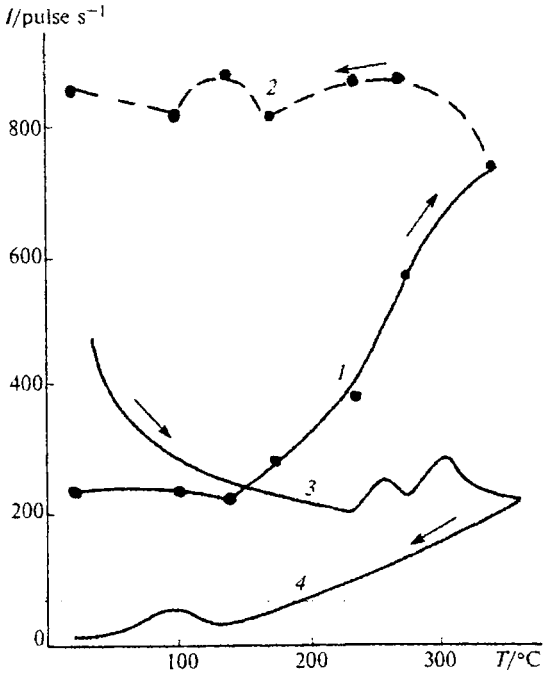

Fig. 5. Temperature dependences of the PSE intensity during stepwise heating (*1*) and cooling (*2*) (shown by arrows) under UVI with λ = 365 nm in the third cycle and PTSE with λ = 365 nm during linear heating (*3*) and cooling (*4*) in the fourth cycle.

PTSE, probably due to the formation of oxide Ce_2O_3 in the surface layer.

To confirm the above conclusions about the centers of PSE from the CeO_2 surface, let us compare the changes in

Table 3. Changes in the PSE intensity (I) in thermocyclic runs with CuO, MnO_2, and CeO_2 at 275 °C and λ = 365 nm

Oxide	I/pulse s^{-1}			T_{red}[a] in H_2 /°C	Reference
	First cycle	Second cycle	Third cycle		
MnO_2	0 → 6	0 → 14[c]	0.5	220 (Mn_3O_4)	17
CuO	30 → 47	0	0	245[d]	23
CeO_2	80 → 170	180 → 420	680 → 880	300 ($CeO_{1.99}$)	5

[a] Arrows indicate an increase in the emission in kinetic runs.
[b] Temperature of reduction. The reduced form is indicated in parenthesis.
[c] A very slow increase in the emission (during 10 min).
[d] Temperature-programmed reduction.

the PSE intensity during thermovacuum and photochemical reduction of transition metal oxides CeO_2, MnO_2, and CuO, which we have previously studied under the same conditions.[14,22] The data characterizing the changes in the intensity of PSE from the samples of these oxides in the thermocyclic experiments are presented in Table 3.

It follows from the data in Table 3 that at 275 °C and under UV1 with λ = 365 nm corresponding to the PSE threshold, the intensity of emission from the MnO_2 and CuO surfaces decreases during the thermovacuum reduction to the background value. This is related to the removal of low-coordinated surface oxygen O^{2-} that forms the PSE centers. At the same time, the intensity of PSE from the CeO_2 surface increases, under these conditions, due to the formation of oxygen vacancies and capability of retaining weakly bound oxygen. The temperatures of reduction of the studied oxides in an H_2 atmosphere are indicated in the last column in Table 3. It has been mentioned[24] that both the chemical reduction and excitation of the charge phototransfer levels occur with electron transfer from the ligand environment to an orbital localized predominantly on the metal ion. According to this, the temperatures of thermovacuum and photochemical treatments resulting in the loss in emission ability of oxides correlates with the temperature of oxide reduction in an H_2 atmosphere.

Thus, the present study shows that the detection of photoemission makes it possible to follow *in situ* the successive stages of thermovacuum reduction under UV1 in the surface layer of oxides.

References

1. W. Liu and M. F. Stephanopoulos, *J. Catal.*, 1995, **153**, 304.
2. W. Liu and M. F. Stephanopoulos, *J. Catal.*, 1995, **153**, 317.
3. K. Otsuka, Y. Wang, E. Sunada, and I. Yamanaka, *J. Catal.*, 1998, **175**, 152.
4. W. Liu, C. Wadia, and M. F. Stephanopoulos, *Catal. Today*, 1996, **28**, 391.
5. L. Kundakovic and M. F. Stephanopoulos, *J. Catal.*, 1998, **179**, 203.
6. H. F. Tuller and A. S. Nowick, *J. Electrochem. Soc.*, 1979, **126**, 209.
7. A. Tshöpe, W. Liu, M. F. Stephanopoulos, and J. Y. Ying, *J. Catal.*, 1995, **157**, 42.
8. C. Li, K. Domen, K.-I. Maruga, and T. Onishi, *J. Am. Chem. Soc.*, 1989, **8**, 7683.
9. I. V. Krylova, *Usp. Khim.*, 1976, **45**, 2138 [*Russ. Chem. Rev.*, 1976, **55** (Engl. Transl.)].
10. I. V. Krylova, *Khimicheskaya Elektronika* [*Chemical Electronics*], Izd-vo MGU, Moscow, 1993 (in Russian).
11. H. Käämbre, *Proc. 17th Karpacz Seminar "Exoemission and Related Phenomena,"* Turava (Poland), 1996, 5.
12. S. R. Morrison, *The Chemical Physics of Surfaces*, Plenum Press, New York–London, 1977.
13. A. A. Lisachenko, Doct. Sci. (Phys.-Math.) Author's Abstract, St. Petersburg State University, St. Petersburg, 1996, 28 pp. (in Russian).
14. I. V. Krylova, *Zh. Fiz. Khim.*, 1998, **72**, 1314 [*Russ. J. Phys. Chem.*, 1998, **72** (Engl. Transl.)].
15. T. V. Simon, Ph. D. (Chem.) Thesis, RKhTU im. D. I. Mendeleeva, Moscow, 1994, 146 pp. (in Russian).
16. I. V. Krylova, *Phys. Stat. Sol. (a)*, 1971, **7**, 359.
17. D. T. Sviridov, R. K. Sviridova, and Yu. F. Smirnov, *Opticheskie spektry ionov perekhodnykh metallov v kristallakh* [*Optical Spectra of Transition Metal Ions in Crystals*], Nauka, Moscow, 1971 (in Russian).
18. J.-M. Hermann, C. Hoang-Van, L. D. Dibansa, and R. Harivololona, *J. Catal.*, 1996, **159**, 361.
19. T. Ito, A. Kawanami, K. Toi, and T. Tokuda, *J. Phys. Chem.*, 1988, **92**, 3910.
20. S. T. Au, A. F. Garley, A. Pashuski, S. Read, M. W. Roberts, and A. Zeini-Isfahan, *Springer Series in Surface Sci.*, 1993, **33**, 241.
21. K. Tanaka and G. J. Blyholder, *J. Chem. Soc., Chem. Commun.*, 1971, 1343.
22. I. V. Krylova, *Zh. Fiz. Khim.*, 2000, **74**, No. 5 [*Russ. J. Phys. Chem.*, 2000, **74**, No. 5 (Engl. Transl.)].
23. Wang Huang Dow, *J. Catal.*, 1996, **160**, 155; 171.
24. D. S. McClure, *Solid State Phys.*, 1996, **9**, 399.

Received June 28, 1999;
in revised form October 18, 1999